Contribution of electron-atom collisions to the plasma conductivity of noble gases

S. Rosmej,[1] H. Reinholz,[1,2] and G. Röpke[1]
[1]*Institut für Physik, Universität Rostock, 18051 Rostock, Germany*
[2]*University of Western Australia, WA 6009 Crawley, Australia*
(Received 17 March 2017; revised manuscript received 1 June 2017; published 29 June 2017)

We present an approach which allows the consistent treatment of bound states in the context of dc conductivity in dense partially ionized noble gas plasmas. Besides electron-ion and electron-electron collisions, further collision mechanisms owing to neutral constituents are taken into account. Especially at low temperatures of 10^4 to 10^5 K, electron-atom collisions give a substantial contribution to the relevant correlation functions. We suggest an optical potential for the description of the electron-atom scattering which is applicable for all noble gases. The electron-atom momentum-transfer cross section is in agreement with experimental scattering data. In addition, the influence of the medium is analyzed, the optical potential is advanced including screening effects. The position of the Ramsauer minimum is influenced by the plasma. Alternative approaches for the electron-atom potential are discussed. Good agreement of calculated conductivity with experimental data for noble gas plasmas is obtained.

DOI: 10.1103/PhysRevE.95.063208

I. INTRODUCTION

Properties of strongly coupled plasmas are of high interest for laser-induced dense plasmas (warm dense matter, WDM) and astrophysical systems. Up to now, the description of such partially ionized plasmas (PIP) is still a challenge because of the quantum-statistical treatment of the electron-atom (*e-a*) collisions in dense matter. In particular, the transport properties are a necessary input parameter for simulation packages. In the present work, the electrical conductivity of dense noble gases is investigated for temperatures of 10^4 to 10^5 K and particle densities below 10^{22} cm^{-3} where the plasma is nonideal and partially ionized.

Fully ionized plasmas (FIP) have been analyzed, starting from the kinetic theory approach, e.g., by Spitzer [1] using a Fokker-Planck equation, as well as by Brooks-Herring [2] or Ziman [3] using the relaxation time approximation, leading to commonly known analytical formulas for the electrical conductivity. The electron-ion (*e-i*) collisions are well described in a wide parameter range, whereas the treatment of *e-a* collisions is not trivial within an analytical approach. Within the linear response theory (LRT), the inclusion of different collision mechanisms is vivid. In recent years, the influence of electron-electron (*e-e*) collisions at arbitrary degeneracy was discussed in Born approximation for a FIP by Reinholz *et al.* [4] and Karakhtanov [5]. In contrast to Spitzer's value, their correction factor depends on density and temperature. Nevertheless, these formulas valid for a FIP are not sufficient for the description of dense partially ionized noble gases, because the interaction with bound states may play an important role.

The treatment of bound states within a quantum-statistical approach is possible if considering a chemical picture. In that case, the electron-ion bound states are identified as a new component (atoms). We consider a PIP containing atoms, free electrons, and singly charged ions. Results for hydrogen are discussed in Refs. [6–8]. For noble gases at temperatures and densities considered here, multiply ionized ions are not relevant. A generalization to multiple ionized states is possible.

For the analysis of *e-a* collisions, the composition of the plasma has to be determined from the mass-action laws. The Saha equation has been studied for a long time by many authors, e.g., Ebeling *et al.* [9,10] and Förster [11] using Padé techniques. As a result, the program package COMPTRA04—for details, see Ref. [12]—allows the calculation of composition and transport properties in nonideal plasmas. It has been successfully applied to metal plasmas; see also Refs. [13,14]. In contrast to this, experimental data for the dc conductivity of noble gases have been understood only qualitatively; see Ref. [15]. A temperature-dependent minimum can be observed as a consequence of the composition, but discrepancies can be up to two orders of magnitude; see Fig. 7 below. Kuhlbrodt *et al.* [15] believe that this results from using the polarization potential for the *e-a* collisions. In Ref. [16], Adams *et al.* verified this statement comparing the calculated momentum-transfer cross sections using a polarization potential with measured data. Subsequently, using the experimental data for the isolated *e-a* momentum-transfer cross section and the composition calculated by COMPTRA04, Adams obtained quantitatively good agreement with experimental results for the dc conductivity of noble gases. Recently, new results from swarm-derived cross sections using different Boltzmann solvers and Monte Carlo simulations have been compared with experimental data for the isolated *e-a* scattering process; see Refs. [17–19]. Especially for low energies, good agreement has been found. However, plasma effects like screening of the *e-a* interaction are not included by using the transport cross sections for isolated collisions.

An alternative to using a polarization potential is the construction of a so-called optical potential [20–23]. Such a potential model has been successfully applied describing the *e-a* momentum-transfer cross sections of all noble gases in a wide energy region; see Ref. [24]. The downside is the large number of free parameters and the fact that a uniform expression for all noble gases has not been available. In this work, we show that a better approximation of the local exchange term leads to a universal expression for the cross section of all noble gases. By adjusting only one free cutoff

parameter r_0 in the polarization term, we find good agreement with the experimental data.

In order to take into account the plasma environment, the optical potential for an isolated collision is further modified by a systematic treatment of statical screening. For a hydrogen plasma, screening of the *e-a* potential within the second order of perturbation, but neglecting the exchange effects, has been discussed by Karakhtanov [25]. Similar characteristics, e.g., a repulsive *e-a* potential at large distances, are found for the noble gases in the present work.

A brief presentation of the fundamental expressions is given in Sec. II. The construction of an optical potential for the *e-a* interaction in dense plasmas is shown in Sec. III and results including a comparison with experimental data are presented in Sec. IV.

II. ELECTRICAL CONDUCTIVITY IN T MATRIX APPROXIMATION

A. Transport properties and equilibrium correlation functions

We start from a systematic quantum statistical approach, the linear response theory (LRT). According to the fluctuation-dissipation theorem, transport coefficients are related to equilibrium correlation functions. For instance, the well-known Kubo formula, see Refs. [26,27], relates the optical conductivity to the current autocorrelation function,

$$\sigma(\omega) = \frac{e^2\beta}{3m^2}\frac{1}{\Omega_\mathrm{N}}\langle \mathbf{P}_1;\mathbf{P}_1\rangle_{\omega+i\varepsilon}\,, \tag{1}$$

with $\beta = 1/(k_\mathrm{B}T)$ (inverse temperature). Due to the large ion mass, only the electron contribution to the current is considered (adiabatic limit), and m is the electron mass. Ω_N denotes the volume of the system containing N_e electrons so that the electron density is $n_\mathrm{e} = N_\mathrm{e}/\Omega_\mathrm{N}$. The current density is

$$\mathbf{j}_\mathrm{e} = \frac{e}{m}\frac{1}{\Omega_\mathrm{N}}\mathbf{P}_1, \text{ and } \mathbf{P}_1 = \sum_k \hbar\mathbf{k}a_k^+a_k \tag{2}$$

is the total momentum of the electrons. a_k^+, a_k, and $a_k^+a_k$ denote the creation, annihilation, and occupation numbers, respectively, of the single-electron state $k = \{\mathbf{k},s\}$ with wave number $\mathbf{k}$ and spin quantum number $s = \pm 1/2$. The autocorrelation function $\langle \mathbf{P}_1;\mathbf{P}_1\rangle_{\omega+i\varepsilon}$ is defined as the Laplace transform according to

$$\langle A;B\rangle_z = \int_0^\infty dt e^{izt}(A(t)|B) \tag{3}$$

of the quantum statistical correlation function given by the Kubo scalar product

$$(A(t)|B) = \int_0^1 d\lambda \mathrm{Tr}\{A(t-i\hbar\beta\lambda)B^\dagger\rho_\mathrm{eq}\}. \tag{4}$$

The average is performed with the equilibrium statistical operator $\rho_\mathrm{eq} = \exp[\beta(H-\mu N)]/\mathrm{Tr}\exp[\beta(H-\mu N)]$, where H is the Hamiltonian of the plasma and μ is the chemical potential. The time dependence $A(t) = \exp[iHt/\hbar]A\exp[-iHt/\hbar]$ is given by the Heisenberg picture. In the classical limit, the expressions for the correlation functions become more simple. They can then be evaluated, e.g., by molecular dynamical (MD) simulations.

Within LRT, alternative expressions to evaluate transport coefficients by equilibrium correlation functions have been derived. They are more appropriate to perform perturbation expansions and to give a connection to the kinetic theory [26,27]. For example, the dc conductivity

$$\sigma(\omega\to 0) \equiv \sigma_\mathrm{dc} = \frac{3e^2n_\mathrm{e}^2}{\beta}\frac{\Omega_\mathrm{N}}{\langle\dot{\mathbf{P}}_1;\dot{\mathbf{P}}_1\rangle_{i\varepsilon}} \tag{5}$$

is related to the force autocorrelation function, $\dot{\mathbf{P}}_1 = (i/\hbar)[H,\mathbf{P}_1]$. In Born approximation, the well-known Ziman formula is obtained. However, to be consistent with kinetic theory and in particular to account for the contribution of *e-e* collisions, we have to include higher moments of the single-particle distribution function (2); see Ref. [8].

Within this paper, we include the third moment $\mathbf{P}_3 = \sum_k \hbar\mathbf{k}(\beta E_k)a_k^+a_k$ which describes the current of heat, and $E_k = \hbar^2k^2/(2m)$. In the low-density limit, the accuracy of this two-moment approximation is better than 3%; see Ref. [8]. The static electrical conductivity can then be expressed by a generalized Ziman formula

$$\sigma = \frac{e^2\beta}{m^2\Omega_\mathrm{N}}\frac{N_{13}^2d_{11}+N_{11}^2d_{33}-2N_{11}N_{13}d_{13}}{d_{11}d_{33}-d_{13}^2}\,, \tag{6}$$

with

$$N_{ll'} = \tfrac{1}{3}(\mathbf{P}_l|\mathbf{P}_{l'})\,, \qquad d_{ll'} = \tfrac{1}{3}\langle\dot{\mathbf{P}}_l;\dot{\mathbf{P}}_{l'}\rangle_{i\varepsilon}\,. \tag{7}$$

The generalized force-force correlation functions $\langle\dot{\mathbf{P}}_l;\dot{\mathbf{P}}_{l'}\rangle_{i\varepsilon}$ contain the generalized forces $\dot{\mathbf{P}}_l = i[H,\mathbf{P}_l]/\hbar = i[V,\mathbf{P}_l]/\hbar$. V denotes the interaction part of the Hamiltonian H.

B. Partially ionized plasmas

There are different tools to evaluate the equilibrium correlation functions occurring in the expressions (1), (5), and (6) for the conductivity of a plasma. Depending on the temperature T and the electron density n_e, the intrinsic structure of the plasma is changing as discussed in Sec. I. The occurrence of bound states (PIP) or the strongly degenerate electron system at very high densities require adequate approaches.

For densities higher than the Mott density, which is in the order of $\approx 10^{23}$ cm^{-3}, the bound states are dissolved. Then at temperatures below $T \sim 10^5$ K, the degeneracy of the electron system is relevant. DFT-MD simulations have been successfully applied to evaluate the correlation functions for these strongly coupled plasmas. Pseudopotentials and structure factor effects are important ingredients under these conditions.

In the present work, we are interested in the density region below the Mott density where neutral atoms are formed. The electrons are nondegenerate but the *e-i* coupling may become large as a prerequisite to form bound states. A suitable approach is the chemical picture. Thus, the ionization degree and the effective *e-a* interaction are important signatures to evaluate the correlation functions. DFT-MD simulations have not yet been successfully applied to particle densities below 10^{22} cm^{-3}.

Within the PIP model (chemical picture) we consider the components $c = \mathrm{e,i,a}$ as individual parts of the plasma with densities n_e, n_i, n_a, respectively, and a heavy particle density $n_\mathrm{heavy} = n_\mathrm{a} + n_\mathrm{i}$. The composition is given by the chemical

equilibrium (Saha equation). An effective Hamiltonian can be constructed for the PIP model:

$$H^{\mathrm{PIP}} = \sum_{c,k} \frac{\hbar^2 k^2}{2m_c} a^+_{k,c} a_{k,c} + \frac{1}{2} \sum_{c,c'} V_{cc'} \,. \tag{8}$$

For our purpose, only the electronic part of the Hamiltonian is of interest:

$$H^{\mathrm{PIP}}_{\mathrm{e}} = \sum_{k} \frac{\hbar^2 k^2}{2m} a^+_k a_k + V_{\mathrm{ei}} + V_{\mathrm{ea}} + \frac{1}{2} V_{\mathrm{ee}} \,. \tag{9}$$

The interaction of electrons with ions and atoms is treated like an external field at fixed positions. Note that, within a Green's function approach, the transition from the fundamental plasma Hamiltonian containing only e and i to the PIP Hamiltonian, Eq. (8), can be made in a systematic way, performing ladder summations and cluster decompositions.

For further discussion, we introduce the coupling parameter

$$\Gamma = \frac{e^2}{4\pi\epsilon_0 k_{\mathrm{B}} T} \left(\frac{4\pi n_{\mathrm{e}}}{3} \right)^{1/3} \tag{10}$$

and the degeneracy parameter

$$\Theta = \frac{2m k_{\mathrm{B}} T}{\hbar^2} (3\pi^2 n_{\mathrm{e}})^{-2/3} \,. \tag{11}$$

Using the plasma conditions given in Sec. I, the electronic subsystem is nondegenerate ($\Theta > 1$) and weakly coupled ($\Gamma < 1$).

C. Evaluation of the generalized force-force correlation functions

Considering the Hamiltonian (9) for the electronic subsystem, the Kubo scalar products in Eq. (7) are evaluated using the Kubo identity, see Refs. [26,27], as

$$N_{11} = \frac{n_{\mathrm{e}} \Omega_{\mathrm{N}} m}{\beta} , \tag{12}$$

$$N_{13} = \frac{5}{2} \frac{n_{\mathrm{e}} \Omega_{\mathrm{N}} m}{\beta} \frac{I_{3/2}(\alpha)}{I_{1/2}(\alpha)} , \tag{13}$$

where $I_\nu(\alpha) = [1/\Gamma(\nu+1)] \int_0^\infty dx\, x^\nu/(1+e^{x-\alpha})$ are the Fermi integrals and $\alpha = \beta\mu_{\mathrm{e}}$ is the temperature-scaled chemical potential of electrons.

After separating the interaction potential into the e-i, e-e, and e-a contributions, Eq. (9), the generalized force-force correlation functions are split into

$$d_{ll'} = d_{l'l} = d^{\mathrm{ei}}_{ll'} + d^{\mathrm{ee}}_{ll'} + d^{\mathrm{ea}}_{ll'} \,, \tag{14}$$

referring to Ref. [4]. Therein, the generalized force-force correlation functions are evaluated in Born approximation using the statically screened Coulomb potential (Debye potential),

$$V_{\mathrm{D}}(r) = -\frac{e^2}{4\pi\epsilon_0} \frac{e^{-\kappa r}}{r} \,, \tag{15}$$

$$\kappa^2 = \kappa_{\mathrm{i}}^2 + \kappa_{\mathrm{e}}^2 = \frac{\beta e^2 n_{\mathrm{e}}}{\epsilon_0} \left[1 + \frac{I_{-1/2}(\alpha)}{I_{1/2}(\alpha)} \right] , \tag{16}$$

for describing the charged particle interaction potentials $V_{\mathrm{ei}}(r) = V_{\mathrm{D}}(r)$ and $V_{\mathrm{ee}}(r) = -V_{\mathrm{D}}(r)$. Note that our quantum statistical approach is not limited by statical screening; the treatment of dynamical screening is possible—see Refs. [5,8,28]. Including strong collisions, the correlation functions are calculated in the T-matrix approximation; see also Refs. [8,29,30]. For $c \neq \mathrm{e}$ we find

$$d^{ec}_{ll'} = \frac{\hbar^3 n_c \Omega_{\mathrm{N}}}{3\pi^2 m} \int_0^\infty dk\, k^5 (\beta E_k)^{\frac{l+l'}{2}-1} f_k (1-f_k) Q^{ec}_{\mathrm{T}}[V_{ec}] \,, \tag{17}$$

with the Fermi distribution function for electrons $f_k = (1 + e^{\beta E_k - \alpha})^{-1}$ and the momentum-transfer cross section

$$Q^{ec}_{\mathrm{T}} = 2\pi \int_{-1}^{1} d(\cos\vartheta)\, [1 - \cos\vartheta] \left(\frac{d\sigma^{ec}}{d\Omega} \right) . \tag{18}$$

Because of momentum conservation, the e-e contributions in d_{1l} vanish: $d^{\mathrm{ee}}_{1l} = 0$. Only the correlation function d_{33} contains e-e collisions explicitly. In the region of partially ionized noble gases, the plasma is nondegenerate ($\Theta > 1$), and the e-e correlation function can be expressed as

$$d^{\mathrm{ee}}_{33} = \frac{8 n_{\mathrm{e}}^2 \Omega_{\mathrm{N}}}{3\sqrt{\pi}\beta} \sqrt{\frac{m}{\beta}} \int_0^\infty dP\, P^7 e^{-P^2} Q^{\mathrm{ee}}_{\mathrm{v}}[V_{\mathrm{ee}}] \,, \tag{19}$$

with the viscosity cross section

$$Q^{\mathrm{ee}}_{\mathrm{v}} = 2\pi \int_{-1}^{1} d(\cos\vartheta)\, [1 - \cos^2\vartheta] \left(\frac{d\sigma^{\mathrm{ee}}}{d\Omega} \right) . \tag{20}$$

More general formulas for d^{ee}_{33} are given in Refs. [4,8]. The cross sections are calculated via the partial wave decomposition ($c = \mathrm{i,a}$)

$$Q^{ec}_{\mathrm{T}}(k) = \frac{4\pi}{k^2} \sum_{\ell=1}^{\infty} \ell \sin^2 \left[\delta^{ec}_{\ell-1}(k) - \delta^{ec}_{\ell}(k) \right] , \tag{21}$$

$$Q^{\mathrm{ee}}_{\mathrm{v}}(k) = \frac{4\pi}{k^2} \sum_{\ell=1}^{\infty} \left[1 + \frac{(-1)^\ell}{2} \right] \frac{\ell(\ell+1)}{2\ell+1} \times \sin^2 \left[\delta^{\mathrm{ee}}_{\ell-1}(k) - \delta^{\mathrm{ee}}_{\ell+1}(k) \right] , \tag{22}$$

with the k-dependent scattering phase shifts $\delta_\ell(k)$. The phase shift calculations are performed using Numerov's method. Recently, the e-i transport cross section has been discussed in detail by Rosmej [31]. In general, at temperatures $T < 10^5$ K, the convergence with respect to the number of relevant phase shifts is fast. The number increases with rising temperature. However, for high temperatures, $T > 10^6$ K, the Born approximation (BA) is applicable ($c \neq \mathrm{e}$):

$$\left(\frac{d\sigma^{ec}}{d\Omega} \right)_{\mathrm{BA}} = \frac{m^2 \Omega_{\mathrm{N}}^2}{4\pi^2\hbar^4} |\tilde{V}(q)|^2 \,, \tag{23}$$

$$\left(\frac{d\sigma^{\mathrm{ee}}}{d\Omega} \right)_{\mathrm{BA}} = \frac{m^2 \Omega_{\mathrm{N}}^2}{16\pi^2\hbar^4} |\tilde{V}(q)|^2 \left(1 - \frac{1}{2} \left| \frac{\tilde{V}(q')}{\tilde{V}(q)} \right| \right) , \tag{24}$$

with the Fourier transformed potential $\tilde{V}(q) = \Omega_{\mathrm{N}}^{-1} \int d^3\mathbf{r}\, e^{i\mathbf{q}\mathbf{r}} V(r)$ and the transferred momenta $q = |\mathbf{q}| = |\mathbf{k} - \mathbf{k}'| = 2k \sin(\vartheta/2)$ and $q' = |\mathbf{q}'| = |\mathbf{k} + \mathbf{k}'| = 2k \cos(\vartheta/2)$.

III. ELECTRON-ATOM INTERACTION IN DENSE PLASMA

A. Optical potential for isolated systems

Within the Green's function technique, the treatment of the *e-a* interaction was expanded up to the second order of perturbation by Redmer *et al.* [32]; see also Ref. [25]

$$V_{\rm ea} = V^{(1)} + V^{(2)} + V_{\rm ex}\,. \tag{25}$$

The nonlocal exchange term $V_{\rm ex}$ had been neglected in Refs. [25,32]. In this work, we consider the role of exchange in a local approximation; see Sec. III B.

The first-order term $V^{(1)}$ describes the Coulomb interaction between the free electron with the nucleus as well as with the shell electrons forming the atom. This part is commonly known as the Hartree-Fock potential $V^{(1)} \equiv V_{\rm HF}(r)$ given by

$$V_{\rm HF}(r) = -\frac{e^2}{4\pi\epsilon_0 r}\int_r^\infty dr_1\, 4\pi r_1 \rho(r_1)(r_1 - r), \tag{26}$$

see also Appendix A, where $\rho(r)$ is the shell electron density in the target atom, which is calculated using the atomic Roothaan-Hartree-Fock wave functions [33]. For large distances, $V_{\rm HF}(r)$ decreases exponentially.

In contrast, the interaction between electrons and neutral particles has been obtained by Born and Heisenberg [34] to be $V_{\rm ea}(r \to \infty) \propto -r^{-4}$ at large distances. Using the Green's function technique, Redmer *et al.* gave the same behavior in the second-order perturbation, which is related to the polarization potential $V^{(2)} \equiv V_{\rm P}$; see Ref. [32]. In the following, we use the polarization potential

$$V_{\rm P}(r) = -\frac{e^2\alpha_{\rm P}}{8\pi\epsilon_0 (r + r_0)^4} \tag{27}$$

as given by Paikeday [35], where $\alpha_{\rm P}$ is the dipole polarizability. r_0 is a cutoff parameter in the order of the Bohr radius a_0 and will be used as a fitting parameter.

In general, the polarization potential depends on the energy of the free electrons. However, Paikeday obtained only a weak energy dependence, which is negligible for our considerations; see Ref. [35]. A number of other analytical expressions for the polarization potential have been suggested before; see Refs. [21,32,36,37]. The cutoff parameter r_0 has also been determined in different ways. In Ref. [32], r_0 was taken to give the correct value for $V_{\rm P}(r = 0)$. Mittleman and Watson [38] derived an analytical formula considering semiclassical electrons, $r_0 = [\alpha_{\rm P} a_0/(2Z^{1/3})]^{1/4}$. Nevertheless, at short distances, the finite value of the polarization term is negligible in contrast to the dominant divergent Coulomb interaction in the Hartree-Fock term. Therefore, it seems to be desirable to choose r_0 to be optimal at intermediate distances. For instance, Paikeday [35] adjusted the cutoff parameter using the experimental data for the differential cross section for *e-a* collisions at intermediate energies. For positron-atom collisions (no exchange part), Schrader adjusted the cutoff parameter using experimental data for the scattering length; see Ref. [37]. The values for their cutoff parameters r_0 are given in Table I, together with our results.

In this work, the cutoff parameter for each noble gas is adjusted in order to reproduce the experimentally determined low-energy behavior of the momentum-transfer cross section, given in Refs. [39] and [40] for helium and neon, respectively. For argon, krypton, and xenon, the so-called Ramsauer-Townsend effect had been experimentally observed for the total cross section by Ramsauer [41] and Townsend [42]. For these heavier noble gases, we chose r_0 using the position and value of the Ramsauer minimum in the momentum-transfer cross section, which were given in Refs. [43–45].

TABLE I. Cutoff parameter r_0 in units of a_0.

$r_0[a_0]$	He	Ne	Ar	Kr	Xe
Present work	1.00	1.00	0.86	0.92	1.00
Mittleman [38]	0.86	0.89	1.21	1.27	1.38
Paikeday [35]	0.92	1.00	2.89	3.40	
Schrader [37]	1.77	1.90	2.23	2.37	2.54

With Eqs. (26) and (27), the *e-a* interaction, Eq. (25), is referred to as the (local) optical potential [20,23]

$$V_{\rm opt}(r) = V_{\rm HF}(r) + V_{\rm P}(r) + V_{\rm ex}(r)\,, \tag{28}$$

if the exchange contribution is approximated by a local field.

B. Approximation of the exchange potential

The exchange contribution in the optical potential, Eq. (28), is considered in a local field approximation. This generally accepted exchange potential was derived in a semiclassical approximation (SCA) [46–48]:

$$V_{\rm ex}^{\rm SCA}[r, K_{\rm RT}(r)] = \frac{\hbar^2}{4m}\left\{K_{\rm RT}^2(r) - \sqrt{K_{\rm RT}^4(r) + \frac{4me^2}{\hbar^2\epsilon_0}\rho(r)}\right\}, \tag{29}$$

with a local electron-momentum $K(r)$, which is here taken in the version of Riley and Truhlar [47,48]

$$K_{\rm RT}^2(r) = k^2 + \frac{2m}{\hbar^2}[|V_{\rm HF}(r)| + |V_{\rm P}(r)|]\,. \tag{30}$$

For a free-electron gas, Mittleman and Watson [49] derived the local exchange potential, see also Ref. [47],

$$V_{\rm ex}^{\rm M}[r, K(r)] = -\frac{e^2}{4\pi\epsilon_0}\frac{2}{\pi}K_{\rm F}(r)F\left(\frac{K(r)}{K_{\rm F}(r)}\right), \tag{31}$$

with the Fermi momentum $K_{\rm F}(r) = [3\pi^2\rho(r)]^{1/3}$ and the function

$$F(\eta) = \frac{1}{2} + \frac{1-\eta^2}{4\eta}\ln\left|\frac{\eta+1}{\eta-1}\right|. \tag{32}$$

Alternatively, Hara [50] included the ionization potential I into the local electron-momentum

$$K_{\rm H}^2(r) = k^2 + 2\frac{2m}{\hbar^2}I + K_{\rm F}^2(r)\,. \tag{33}$$

When inserting $K(r) = K_{\rm H}(r)$ in Eq. (31), the exchange term is labeled as Hara's free-electron-gas exchange approximation (FEH). It has been discussed by Hara as well as by Riley

TABLE II. e-He, e-Ne, and e-Ar partial wave phase shifts δ_ℓ (in rad) for $\ell = 0,1,2$ omitting the polarization term, $V_P = 0$, in the optical potential, Eq. (28). (1) Numerical results in static-exchange approximation (SEA), Refs. [51–53]; (2) present work (RRR), Eq. (31) with (34); (3) semiclassical exchange approximation (SCA), Eq. (29); (4) Hara's free-electron-gas exchange approximation (FEH), Eq. (31) with (33); and (5) Riley-Truhlar's free-electron-gas exchange approximation (FER), Eq. (31) with (30).

Helium			δ_0					δ_1					δ_2		
ka_0	(1)	(2)	(3)	(4)	(5)	(1)	(2)	(3)	(4)	(5)	(1)	(2)	(3)	(4)	(5)
0.10	2.994	2.993	3.006	2.957	3.337										
0.25	2.776	2.770	2.783	2.691	3.043										
0.50	2.436	2.412	2.422	2.304	2.648	0.043	0.045	0.076	0.023	0.218					
0.75	2.139	2.093	2.111	2.001	2.332	0.110	0.101	0.146	0.064	0.316	0.005	0.006	0.009	0.004	0.013
1.00	1.890	1.835	1.856	1.769	2.071	0.183	0.159	0.205	0.116	0.359	0.014	0.015	0.020	0.010	0.025
1.50	1.522	1.473	1.491	1.446	1.654	0.284	0.247	0.279	0.212	0.367	0.042	0.041	0.047	0.035	0.053
Neon			δ_0					δ_1					δ_2		
ka_0	(1)	(2)	(3)	(4)	(5)	(1)	(2)	(3)	(4)	(5)	(1)	(2)	(3)	(4)	(5)
0.20	6.072	6.104	6.179	6.028	7.716										
0.30	5.965	6.004	6.069	5.902	7.056										
0.40	5.857	5.899	5.947	5.779	6.648										
0.50	5.748	5.789	5.820	5.659	6.361	3.040	3.052	3.030	2.917	3.196	0.004	0.005	0.008	0.002	0.016
0.70						2.933	2.949	2.909	2.785	3.124					
0.80						2.873	2.890	2.845	2.724	3.073					
0.90	5.321	5.349	5.333	5.215	5.626	2.812	2.828	2.781	2.667	3.017					
1.00	5.219	5.243	5.222	5.114	5.480	2.751	2.766	2.719	2.615	2.958	0.065	0.059	0.075	0.034	0.127
Argon			δ_0					δ_1					δ_2		
ka_0	(1)	(2)	(3)	(4)	(5)	(1)	(2)	(3)	(4)	(5)	(1)	(2)	(3)	(4)	(5)
0.10	9.274	9.266	9.374	9.249	11.858	6.279	6.276	6.279	6.275	6.318					
0.25	9.045	9.015	9.141	8.987	10.628	6.227	6.193	6.213	6.192	6.381	0.002	0.002	0.004	0.001	0.031
0.50	8.647	8.580	8.658	8.561	9.250	6.001	5.901	5.938	5.909	6.214	0.045	0.035	0.061	0.024	0.815
0.75	8.249	8.164	8.206	8.162	8.536	5.702	5.583	5.613	5.604	5.901	0.277	0.185	0.284	0.150	1.963
1.00	7.875	7.790	7.808	7.798	8.030	5.411	5.305	5.320	5.333	5.575	0.860	0.581	0.782	0.536	2.008
1.50	7.252	7.170	7.163	7.182	7.288	4.923	4.861	4.854	4.892	4.996	1.644	1.539	1.614	1.594	1.877

and Truhlar [47] that $K_H(r)$ leads to a wrong asymptotic behavior of the exchange potential for large distances. Some modifications have been suggested in Refs. [22,47]. Riley and Truhlar discussed Eq. (30) for the local electron momentum. After inserting $K(r) = K_{RT}(r)$ in Eq. (31), the exchange term is labeled as Riley-Truhlar's free-electron-gas exchange approximation (FER).

In this work, we suggest a modification of the local electron momentum of Riley and Truhlar, Eq. (30), by adding the momentum-free exchange term $V_{ex}^{M}(r,0) = -\frac{e^2}{4\pi\epsilon_0}\frac{2}{\pi}K_F(r)$, leading to

$$K_{RRR}^2(r) = k^2 + \frac{2m}{\hbar^2}\left[|V_{HF}(r)| + |V_P(r)| + \left|V_{ex}^{M}(r,0)\right|\right]. \tag{34}$$

For verification of our proposed optical potential, we consider a numerical solution of the scattering problem in first order of perturbation, which has been neglecting polarization effects. The scattering phase shifts have been calculated within a static-exchange approximation (SEA) using a nonlocal exchange term; see Refs. [51–53]. For a consistent comparison, we performed our calculation omitting the polarization potential ($V_P = 0$) in Eqs. (28), (30), and (34). In Table II, the results of the phase shift calculations for different proposed local exchange potentials are shown in comparison to the numerical results for the nonlocal exchange term. The latter calculations have been performed by Duxler *et al.* [51] for helium, by Thompson [52] for neon and argon, and by Pindzola and Kelly [53] for argon.

For helium, argon, and neon, we obtain that FEH underestimates and FER overestimates the effect of exchange. This is in accordance with Riley and Truhlar's calculations for helium and argon; see Ref. [47]. Both expressions, FEH and FER, are not satisfying for the treatment of the exchange part. The frequently used SCA, Eqs. (29) and (30), as well as the present work (denoted as RRR), Eqs. (31) and (34), are in good agreement with the SEA phase shifts. Note that for high wave numbers $ka_0 \gg 1$, both potentials, SCA and RRR, have the same asymptotic behavior. For small wave numbers $ka_0 \leqslant 0.5$, the proposed RRR leads to the best results, with an error of $\leqslant 0.1$ rad. This is relevant for the different characteristics in the momentum-transfer cross sections. For instance, the simple structure for helium as well as the shoulder in neon, see Fig. 2 below, are influenced by the exchange part.

For the determination of the optimal value of the parameter r_0 in the polarization term, Eq. (27), as explained at the end of the previous subsection, the calculation of the e-a momentum-transfer cross section, Eq. (21), has been performed for the full optical potential, Eq. (28), including the polarization term, Eq. (27), as well as with the polarization potential in the exchange term, Eq. (31) with (34). As a result, the values given in Table I above are obtained.

C. Plasma effects

As a dominant plasma effect on the electron-atom interaction, we now discuss the screening of each term of the optical potential,

$$V^{\rm s}_{\rm opt}(r) = V^{\rm s}_{\rm HF}(r) + V^{\rm s}_{\rm P}(r) + V^{\rm s}_{\rm ex}(r)\,. \tag{35}$$

The effect of the plasma on the polarization potential was already extensively investigated. A screening factor was suggested by Redmer and Röpke [54]

$$V^{\rm s}_{\rm P}(r) = V_{\rm P}(r)\, e^{-2\kappa r}(1+\kappa r)^2\,, \tag{36}$$

with the screening parameter κ defined in Eq. (16), which will be used in our calculations.

For the screened Hartree-Fock term, the Coulomb interaction in Eq. (26) for the isolated system can be replaced by a Debye potential. For partially ionized hydrogen plasma, this was done by Karakhtanov [25]. In Appendix A, we have derived the following expression:

$$V^{\rm s}_{\rm HF}(r) = \frac{e^2}{4\pi\epsilon_0}\left[-\frac{Ze^{-\kappa r}}{r} + I_1 + I_2 + I_3\right], \tag{37}$$

$$I_1 = \frac{e^{-\kappa r}}{\kappa r}\int_0^r 2\pi r_1 \rho(r_1) e^{\kappa r_1}\, dr_1\,, \tag{38}$$

$$I_2 = -\frac{e^{-\kappa r}}{\kappa r}\int_0^\infty 2\pi r_1 \rho(r_1) e^{-\kappa r_1}\, dr_1\,, \tag{39}$$

$$I_3 = \frac{e^{\kappa r}}{\kappa r}\int_r^\infty 2\pi r_1 \rho(r_1) e^{-\kappa r_1}\, dr_1\,, \tag{40}$$

where Z is the charge number of the nucleus. The asymptotic behavior of the screened Hartree-Fock term, Eq. (37), is derived in Appendix B. Note that at large distances, $r \to \infty$, it becomes repulsive. For intermediate screening parameters $0 < \kappa a_0 < 1$, expression

$$V^{\rm s}_{\rm HF}(r) = \frac{Ze^2}{4\pi\epsilon_0}\frac{e^{-\kappa r}}{r}\,\mathcal{C}_0\left[(\kappa a_0)^2 + \mathcal{O}(\kappa^4)\right], \tag{41}$$

$$\mathcal{C}_0 = \frac{Z^{-1}}{6}\int_0^\infty \left(\frac{r_1}{a_0}\right)^2 4\pi r_1^2 \rho(r_1)\, dr_1\,, \tag{42}$$

can be used. $\mathcal{C}_0$ is an element-specific constant; see Table III in Appendix A for the noble gases. For hydrogen, the exact value is $\mathcal{C}_0^{\rm H} = 1/2$.

For the screened exchange term in Eq. (35), we replace the Hartree-Fock and polarization term in Eq. (34) by their screened versions, Eq. (36) and Eq. (37), respectively.

In the unscreened case, Eq. (28), the polarization term is the main contribution to the optical potential at large distances, regardless of the chosen Hartree-Fock term. For the screened optical potential, Eq. (35), the Hartree-Fock term is dominant, and the screened optical potential becomes repulsive, for all noble gases. Karakhtanov [25] obtained the same asymptotic behavior for partially ionized hydrogen.

Exemplarily, the screened optical potential, Eq. (35), for the e-Ar interaction is shown in Fig. 1. Beside the isolated case ($\kappa a_0 = 0$), the potential is calculated at the plasma conditions $\kappa a_0 = 0.05$ and 0.1. For a temperature of 20 000 K, this is related to heavy particle densities $n_{\rm heavy} = 1.9 \times 10^{20}{\rm cm}^{-3}$ and $1.5 \times 10^{21}{\rm cm}^{-3}$, respectively. At large distances, the screened optical potential can be approximated by the asymptotic Hartree-Fock term, Eq. (41). The e-Ar potential becomes repulsive. At short distances, the plasma surrounding can be neglected, and screening effects are not relevant. A similar behavior is obtained for all other noble gases as well.

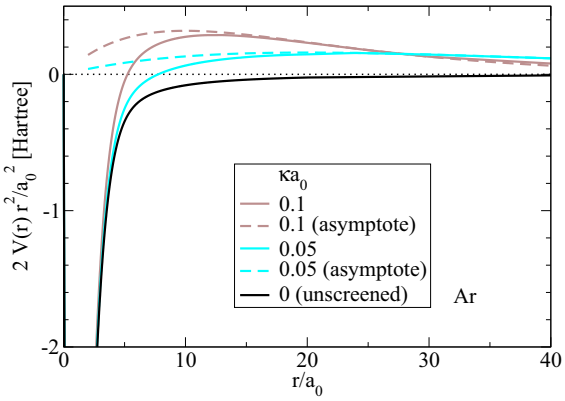

FIG. 1. Screened optical potential, Eq. (35), for electron-argon interaction at zero wave number ($k = 0$) for different screening parameters κa_0 in comparison to the unscreened optical potential, Eq. (28). The asymptotes, Eq. (41), are also shown.

IV. RESULTS

A. Momentum-transfer cross section

The momentum-transfer cross sections for the electron-atom interaction of noble gases, Eq. (21), for isolated collisions are calculated using the phase shifts for the optical potential, Eq. (28), with Eqs. (26), (27), (31), and (34). The results are shown in Fig. 2, in comparison to experimental data for He [39,55–57], Ne [40,57,58], Ar [43,57,59–61], Kr [44,61,62], and Xe [45,63,64] as well as results from theoretical calculations [24].

We observe an overall good agreement between our calculations and the measured data. We find that the simple behavior in the case of helium as well as the more complex structure of the momentum-transfer cross section for the other noble gases is well described by the optical potential given here. For low and intermediate energies, the shoulder for neon [40] as well as the Ramsauer minimum obtained for argon [43], krypton [44], and xenon [45] are reproduced. Deviations between calculated and measured values at larger values of the wave number k are found for argon and krypton. These discrepancies may be resolved by further experimental and theoretical investigations.

The results by Adibzadeh and Theodosiou [24], see Fig. 2, are from calculations using a different optical potential. For each element, exchange and polarization potential are specifically constructed adjusting four parameters. In our approach, this large number of fitting parameters is not required. Based on a general form of the exchange potential, the cutoff parameter r_0 for the polarization potential, Eq. (27), is the only parameter fitted to element specific data; see Table I. The maximum

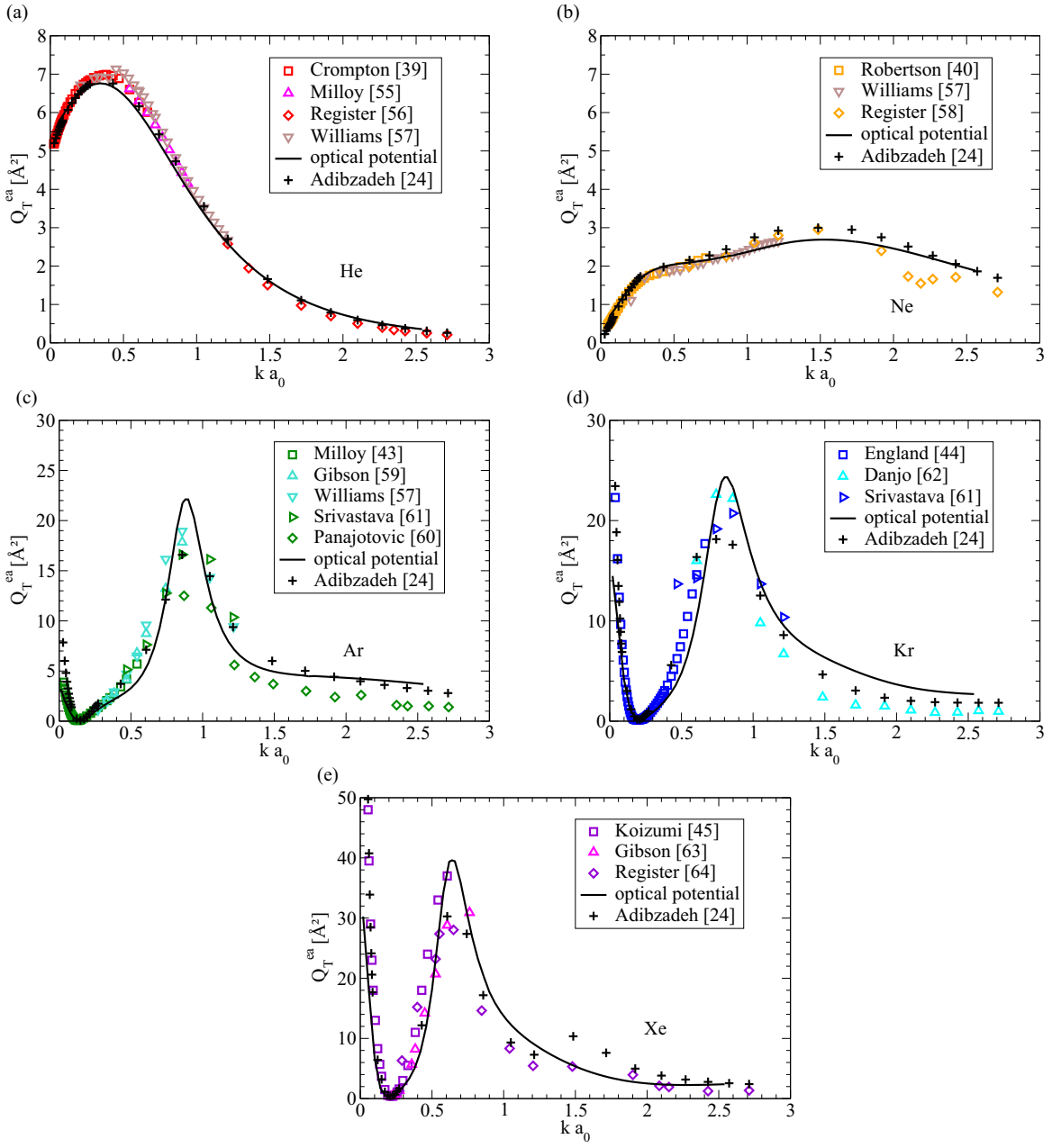

FIG. 2. Momentum-transfer cross section for the noble gases: (a) He, (b) Ne, (c) Ar, (d) Kr, and (e) Xe. The calculations are performed using the optical potential Eq. (28) in the present work (full line), Eqs. (26), (27), (31), and (34), in comparison with the optical potential used in [24] (crosses). Also shown are experimental data [39,40,43–45,55–64].

near $ka_0 \approx 0.8$ for the heavier noble gases argon, krypton, and xenon, as calculated by Adibzadeh and Theodosiou, is lower than the maximum obtained from our optical potential. This difference can be explained by the different choice of the exchange and polarization term.

B. Screening effects on the momentum-transfer cross section

In the following, we discuss the effect of the plasma environment on the momentum-transfer cross section $Q_T^{ea}(k)$ for the electron-atom interaction of noble gases, Eq. (21), calculating the phase shifts for the screened optical potential, Eq. (35), with Eqs. (36) and (37). Figure 3 shows the results for helium and argon. As also known from the *e-i* interaction, the plasma environment affects the transport of slower electrons more than faster ones.

First we consider argon; see Fig. 3(a). For increasing screening parameters κa_0, see inset, the momentum-transfer cross section for slow electrons drops rapidly. Reaching $\kappa a_0 \approx 0.025$, the Ramsauer minimum is dissolved. This is a consequence of the decreasing zeroth scattering phase shift for the screened optical potential in contrast to the isolated system $\delta_0^{\text{screened}}(k) < \delta_0^{\text{isolated}}(k)$. Up to this screening parameter, discrepancies of the momentum-transfer cross section between the isolated system and the plasma are still negligible for intermediate and high energies ($ka_0 \gtrsim 0.2$).

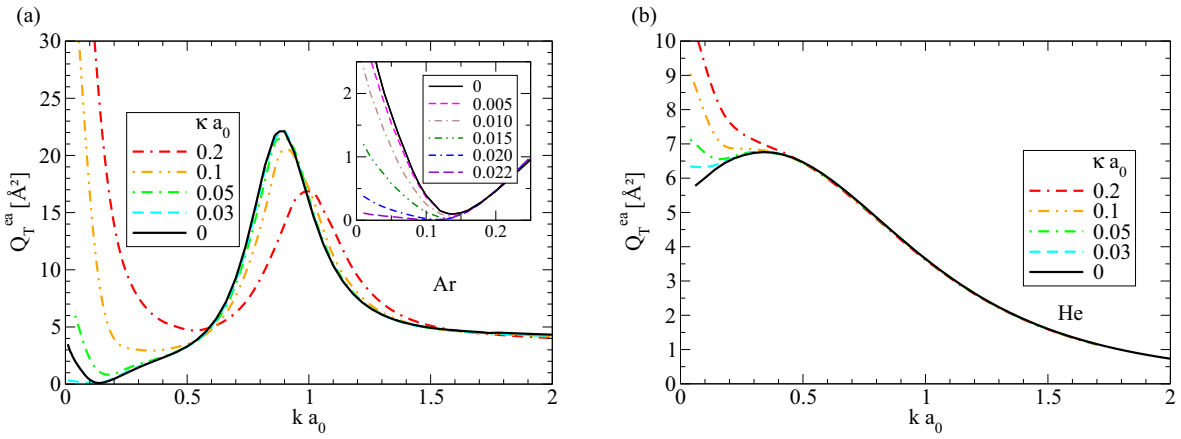

FIG. 3. Screening effects on the momentum-transfer cross section for (a) argon and (b) helium at various screening parameters κ.

For dense plasmas, $\kappa a_0 > 0.025$, the then repulsive screened optical potential reduces the zeroth scattering phase shift to $\delta_0(k) < 3\pi$. The Ramsauer minimum stays dissolved, the momentum-transfer cross section increases. A new minimum, which appears in the momentum-transfer cross section, is a result of phase shifts for higher l which is not the Ramsauer effect. The depth of the minimum rises with the screening parameter κ, and the minimum's position shifts to higher energies. Furthermore, the maximum's position is also shifted to higher energies and the height itself decreases. The same principle behavior is also obtained for krypton and xenon.

Now, we consider helium; see Fig. 3(b). The scattering phase shifts for the screened optical potential are smaller than for the isolated system. Because of $\delta_0^{\text{screened}} < \delta_0^{\text{isolated}} < \pi$, the momentum-transfer cross section increases for rising screening parameters κ. A minimum appears in the momentum-transfer cross section as a consequence of the first scattering phase shift δ_1. Similar to argon, for stronger screening parameters κ, the minimum's depth increases and its position shifts to higher energies. At $\kappa a_0 \approx 0.1$, the minimum changes to a saddle point and for further increasing screening parameters κ an inflection point is obtained. For neon, we obtain a similar behavior as for helium.

C. Correlation functions

For partially ionized systems, the composition has to be known to calculate the influence of the electron-atom contribution. The composition of the noble gases for a given temperature T and a mass density ρ was calculated with COMPTRA04 [12].

As an example again, the ionization degree $\alpha_{\text{ion}} = n_e/n_{\text{heavy}}$ in dependence on the heavy particle density $n_{\text{heavy}} = \rho N_A/M = n_a + n_i$, in Fig. 4(a), and on the degeneracy parameter Θ, in Fig. 4(b), is shown at $T = 20\,000$ K. At low densities, the plasma is fully ionized, $n_a \approx 0$, with singly charged ions, $\alpha_{\text{ion}} \approx 1$. For intermediate densities, the ionization degree develops a minimum. For high densities, bound states are dissolved by the Mott effect, and the plasma becomes fully ionized $n_a \approx 0$. This behavior of the ionization degree is characteristic for other temperatures, too. The strength and the position of the minimum depends on the temperature. For lower temperatures, the fraction of atoms is higher; see Ref. [7].

Knowing the composition of the plasma and the different contributions to the momentum-transfer cross section, the correlation functions have been calculated using the formulas, Eqs. (17) and (19), given in Sec. II C. For $T = 20\,000$ K, the correlation functions d_{11}/d and d_{33}/d are shown in Figs. 5(a) and 5(b), respectively, where

$$d = \frac{4}{3}\sqrt{2\pi m\beta}[(n_e e^2)/(4\pi\epsilon_0)]^2\Omega_N. \tag{43}$$

The different contributions (e-i, e-a, and e-e) are presented separately for comparison. As implied in Fig. 4, the atomic contribution is most relevant at the minimum of the ionization degree and becomes weaker for higher densities as a consequence of the Mott effect. Despite the small ionization degrees at intermediate densities, the charged particle contributions to the correlation functions are dominant, e.g., at $\Theta > 1000$ for helium and $\Theta > 100$ for neon. This fact can be explained by the weakness of the e-a interaction in contrast to the charged

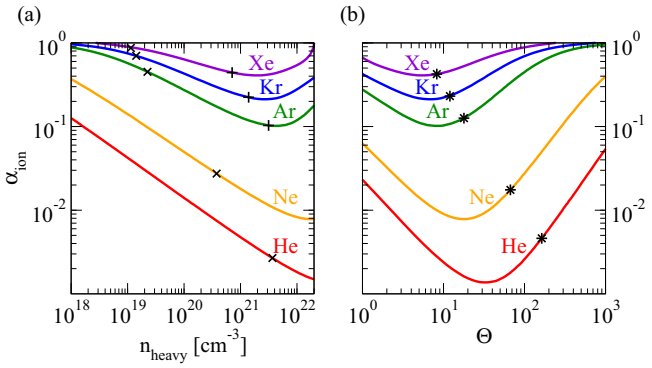

FIG. 4. Ionization degree of partially ionized noble gases at $T = 20\,000$ K according to Ref. [12] (a) as a function of n_{heavy}, × indicates the value of $\Theta = 100$, + the value $\Theta = 10$; and (b) as a function of Θ, ∗ indicates the value $n_{\text{heavy}} = 10^{21}$ cm^{-3}.

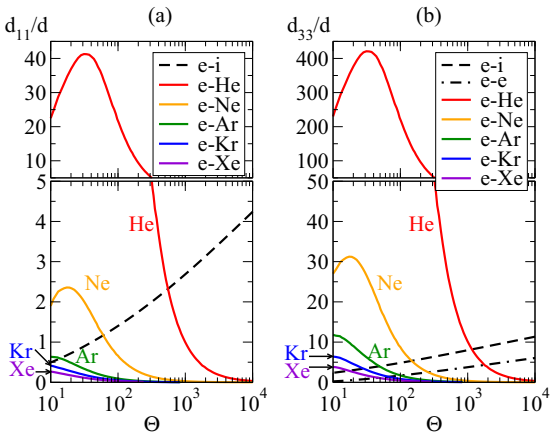

FIG. 5. Correlation functions (a) d_{11} and (b) d_{33} relative to d, Eq. (43), for the different considered scattering mechanisms *e-i* (dashed line), *e-e* (dash-dotted line), and *e-a* (full lines) at $T = 20\,000$ K (two scales).

particle interaction. Note for this that the correlation functions are given in terms of d, see Eq. (43), which contain the particle densities. The *e-e* contribution is explicitly given in d_{33}; see Sec. II. In the low-density limit, the ratio between *e-i* and *e-e* contributions is $d_{33}^{ei}/d_{33}^{ee} \to \sqrt{2}$. With increasing density, the *e-e* contribution can be neglected because of the Pauli blocking (see Ref. [4]); only the ionic contribution is important. In this highly degenerated limit, $\Theta \ll 1$, the Ziman formula is applicable for the calculation of the conductivity. Figures 4 and 5 are analyzed as examples. Similar results are obtained for partially ionized plasmas at temperatures of $T = 10^4$ to 10^5 K; see Refs. [7,15]. Above these temperatures, the plasma can be described by a fully ionized plasma. At lower temperatures, in the region of condensed matter densities, i.e., $\Gamma > 3$, the formulas in Sec. II should be extended including the ionic and atomic structure factors.

D. Electrical conductivity for partially ionized noble gases

The electrical conductivity for the noble gases is now determined using Eq. (6) with the correlation functions according to Eqs. (12), (13), (17), and (19). The results are presented in dependence on the heavy particle density n_{heavy}; see Figs. 6 and 7.

In Fig. 6, the conductivity at a temperature of $T = 20\,000$ K is shown considering several orders of magnitude for the particle density. A characteristic minimum, which is also known for hydrogen (see Refs. [7,25]) is observed for all noble gases at densities where the ionization degree is the lowest. In Fig. 6(a), the conductivity assuming a fully ionized plasma (dash-dotted line) as well as a partially ionized plasma with neglected *e-a* collisions (dashed line) are shown for comparison. Because of the reduced number of charge carriers, the ionization itself already leads to a lower conductivity. The further strong reduction of the conductivity is a consequence of *e-a* collisions. Corresponding to Figs. 4 and 5, the effect is stronger for the lighter elements. As can be seen, the experimental data are well described by the PIP using our optical potential. Similarly good agreement was found by Adams *et al.* [16], who used the experimental momentum-transfer cross sections for isolated *e-a* collisions. Note that the screening parameters at the experimental conditions are small, $\kappa a_0 \leqslant 0.1$. Therefore, the influence of the plasma environment on the *e-a* collisions due to screening is weak. The effect on the conductivity is smaller than 5%.

In Fig. 7, the conductivity of argon and xenon is shown in dependence on n_{heavy} at three temperatures. For comparison with experimental data, calculations for the particular experimental conditions are shown as separate points too. The agreement is within the experimental uncertainty. Calculations by Kuhlbrodt *et al.* [15] were performed using COMPTRA04. Note that for the transport properties, the polarization potential is implemented for the description of *e-a* collisions. The results are up to two orders of magnitude lower than the experimental data. This supports our finding that the polarization potential is not sufficient for the description of *e-a* collisions in

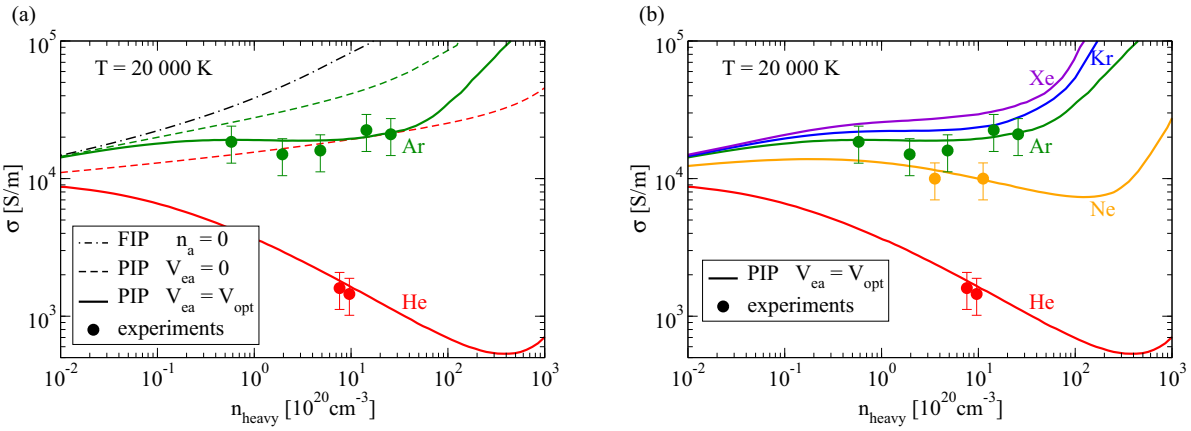

FIG. 6. Conductivity of partially ionized noble gases (PIP) using the optical potential for the *e-a* interaction (full lines): (a) helium (red) and argon (green) at 20 000 K in comparison with experimental data (•[65–67]), fully ionized plasma (FIP) model $n_a = 0$ (dash-dotted lines) and neglecting *e-a* interaction $V_{ea} = 0$ (dashed lines); and (b) helium (red), neon (orange), argon (green), krypton (blue), and xenon (violet) at 20 000 K in comparison with the experimental data (•[65–67]).

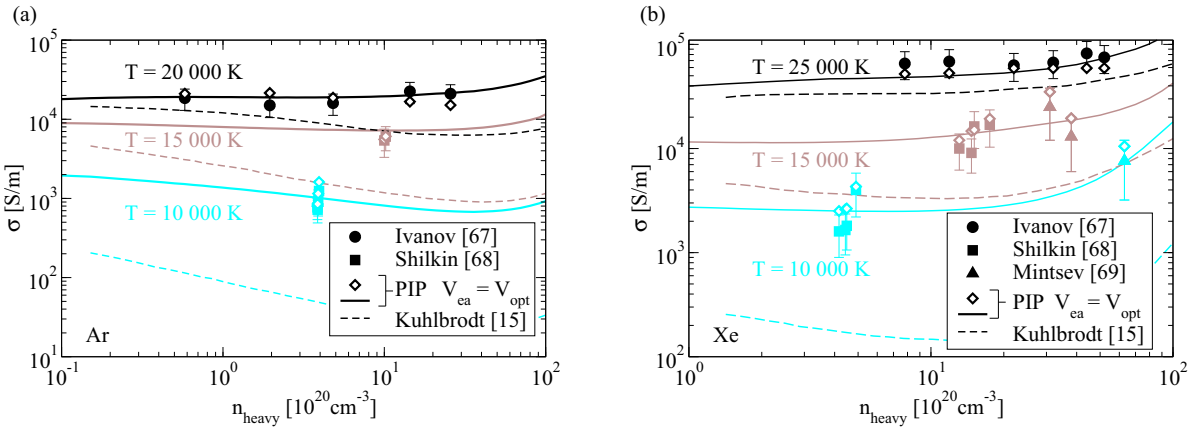

FIG. 7. Conductivity of partially ionized noble gases (PIP) using the optical potential for the *e-a* interaction (full lines): (a) argon at temperatures $T = 10\,000$ K (cyan), 15 000 K (brown), and 20 000 K (black) in comparison with calculations using the polarization potential [15] (dashed line) and experimental data around these temperatures [67,68] (•, Ref. [67]; ■, Ref. [68]; and ◊, calculations at experimental conditions); and (b) xenon at temperatures $T = 10\,000$ K (cyan), 15 000 K (brown), and 25 000 K (black) in comparison with calculations using the polarization potential [15] (dashed) and experimental data around these temperatures [67–69] (•, Ref. [67]; ■, Ref. [68]; ▲, Ref. [69]; and ◊, calculations at experimental conditions).

noble gases. Nevertheless, the qualitative behavior of the conductivity, e.g., the characteristic minimum, is also observed by Kuhlbrodt *et al.* [15].

V. CONCLUSION

Within the LRT, general expressions for the transport properties of partially ionized plasmas are obtained starting from a quantum-statistical approach. The chemical picture can be introduced in a systematic way by performing partial summations of ladder diagrams; see Ref. [70]. Atoms (bound states) are considered as a new species, and the composition given by the ionization equilibrium is calculated taking many-particle effects into account. Semiempirical expressions for the effective potentials, in particular for the *e-a* interactions, can be derived by first-principle approaches.

We have introduced an optical potential to describe the *e-a* interaction. A more systematic approach using the Green's function method would give an interaction which is nonlocal and energy dependent. The optical potential used in this work is motivated by the perturbation theory up to second order, which combines the Coulomb interaction relevant at short distances and the polarization potential relevant at large distances. The exchange contribution is given by an effective local field, which is determined by the condition that the characteristic scattering phase shifts of the nonlocal first-order perturbation theory, the static-exchange approximation, are reproduced. The many-particle approach using the method of Green's functions can be used to find systematic improvements of the effective interaction model applied in the present work.

We have show that a uniform expression for the optical potential can be introduced to describe the momentum-transfer cross section for all noble gases with high precision. Just one parameter r_0 is adjusted, describing the *e-a* scattering mechanism. If going beyond the Born approximation, specific effects, e.g., the Ramsauer-Townsend minimum, appear within the T-matrix approach.

The optical potential model is extended to describe dense plasma environment in which screening is relevant. The effect on the momentum-transfer cross sections has been discussed. In particular, we have shown that the Ramsauer-Townsend minimum is modified by plasma effects and might dissolve, depending on the plasma parameter. Furthermore, the electrical conductivity is calculated for plasma conditions $T = 10^4$ to 10^5 K and $n_{\text{heavy}} \lesssim 10^{22}\,\text{cm}^{-3}$. The results are in good agreement with experimental data. We found that screening effects only have a small influence on the conductivity in the considered parameter region. The relative changes are smaller than 5%. This explains why the calculations for the conductivity using the experimental momentum-transfer cross sections of isolated atoms [16] are already in reasonable agreement with the measured data for partially ionized plasmas.

In general, if exploring WDM as well as ultracold gases, the medium (plasma) effects may become more relevant for the description of transport properties. For future work, dynamical screening, the Pauli blocking, the static structure factor and degeneracy effects on the quantum mechanical T matrix could be treated within our quantum-statistical approach. At increasing densities ($\sim 10^{23}$ cm^{-3}), the Mott effect describes the dissolution of the bound states. Then, other aspects may become of relevance. Exchange and pseudopotential effects are consistently described by DFT-MD and PIMC approaches; see Refs. [71,72]. However, in the region below the Mott density considered in the present work, DFT calculations are very cumbersome and need further improvements to give good results for partially ionized plasmas. Here, as shown in the present work, the PIP model describing a multicomponent plasma with effective interactions allows for an efficient and accurate treatment of transport properties, such as the dc conductivity.

ACKNOWLEDGMENTS

The authors acknowledge support from the Deutsche Forschungsgemeinschaft (DFG) within the Collaborative Research Center SFB 652.

APPENDIX A: SCREENED HARTREE-FOCK POTENTIAL

The Hartree-Fock potential between an electron and an atom describes the Coulomb interaction between the incoming electron with the core and the shell electrons given by

$$V_{\rm HF}(r) = \frac{e^2}{4\pi\epsilon_0}\left[-\frac{Z}{r} + \int \frac{1}{|\mathbf{r}-\mathbf{r_1}|}\rho(r_1)\,d^3\mathbf{r_1}\right], \quad \text{(A1)}$$

which is identical to Eq. (26), where the charge number of the nucleus is expressed as $Z = \int d^3\mathbf{r}'\rho(r') = \int_0^\infty dr' 4\pi r'^2\rho(r')$ and $\rho(r)$ is the density of the shell electrons.

For the plasma system, we replace the Coulomb interaction by a Debye potential

$$V^{\rm s}_{\rm HF}(r) = \frac{e^2}{4\pi\epsilon_0}\left[-\frac{Ze^{-\kappa r}}{r} + \int \frac{e^{-\kappa|\mathbf{r}-\mathbf{r_1}|}}{|\mathbf{r}-\mathbf{r_1}|}\rho(r_1)\,d^3\mathbf{r_1}\right]. \quad \text{(A2)}$$

The second term in the square brackets can be written as

$$2\pi\int_0^\infty dr_1\, r_1^2\rho(r_1)\int_{-1}^1 dz\,\frac{e^{-\kappa\sqrt{r^2+r_1^2-2rr_1z}}}{\sqrt{r^2+r_1^2-2rr_1z}}.$$

By substituting $y = \sqrt{r^2+r_1^2-2rr_1z}$, we obtain

$$2\pi\int_0^\infty dr_1\, r_1^2\rho(r_1)\int_{|r-r_1|}^{r+r_1} dy\,\frac{e^{-\kappa y}}{rr_1}.$$

By performing the integral over y, we can split the integral over r_1 into three contributions. Finally, we obtain Eq. (37).

APPENDIX B: ASYMPTOTIC BEHAVIOR FOR THE SCREENED HARTREE-FOCK POTENTIAL

Expanding the exponential functions in the integrand of I_1 and I_2 [see Eqs. (38) and (39), respectively], we obtain

$$I_1 = \frac{e^{-\kappa r}}{\kappa r}\int_0^r 2\pi r_1\rho(r_1)\left\{1+\kappa r_1 + \frac{\kappa^2 r_1^2}{2} + \cdots\right\}dr_1, \quad \text{(B1)}$$

$$I_2 = -\frac{e^{-\kappa r}}{\kappa r}\int_0^\infty 2\pi r_1\rho(r_1)\left\{1-\kappa r_1 + \frac{\kappa^2 r_1^2}{2} - + \cdots\right\}dr_1, \quad \text{(B2)}$$

TABLE III. Coefficients $\mathcal{C}_k$ in Eq. (B5) for noble gases.

k	$\mathcal{C}_k^{\rm He}$	$\mathcal{C}_k^{\rm Ne}$	$\mathcal{C}_k^{\rm Ar}$	$\mathcal{C}_k^{\rm Kr}$	$\mathcal{C}_k^{\rm Xe}$
0	0.1974	0.1563	0.2411	0.1830	0.1933
1	0.0324	0.0228	0.0672	0.0568	0.0727
2	0.0050	0.0033	0.0170	0.0165	0.0262
3	0.0007	0.0005	0.0044	0.0044	0.0088
4	0.0001	0.0001	0.0013	0.0011	0.0028

$$I_1 + I_2 > \frac{Ze^{-\kappa r}}{r} - \frac{e^{-\kappa r}}{\kappa r}\int_r^\infty 2\pi r_1\rho(r_1)\left\{1+\kappa r_1+\kappa^2 r_1^2\right\}. \quad \text{(B3)}$$

For large distances $r\to\infty$, I_3 in Eq. (40) is larger than the last term in Eq. (B3), so that $V_{\rm HF}(r)$ becomes repulsive.

With $I_1 = \int_0^r dr_1 ... = \int_0^\infty dr_1 ... - \int_r^\infty dr_1 ...$, we find

$$V^{\rm s}_{\rm HF}(r) = \frac{e^2}{4\pi\epsilon_0}\frac{e^{-\kappa r}}{r}\int_0^\infty 4\pi r_1^2\rho(r_1)\left\{\frac{\kappa^2 r_1^2}{3!} + \frac{\kappa^4 r_1^4}{5!} + \cdots\right\}dr_1 - \frac{e^2}{4\pi\epsilon_0}\frac{1}{\kappa r}\int_r^\infty \frac{\rho(r_1)}{r_1}\sinh[\kappa(r_1-r)]\,dr_1. \quad \text{(B4)}$$

Since the lower boundary in the second term is r itself and the shell electron density $\rho(r)$ is zero for distances larger than the atomic radius, the leading term, for $r\to\infty$, is of the order $\mathcal{O}(e^{-r/a_0})$ or weaker; see Ref. [33]. The first term in Eq. (B4) is in the order of $O(e^{-\kappa r}/r)$. In the limit of $\kappa < 1/a_0$, the second term can therefore be neglected. The first term can be expanded in terms of $(\kappa a_0)^2$:

$$\lim_{r\to\infty} V^{\rm s}_{\rm HF}(r) = \frac{Ze^2}{4\pi\epsilon_0}\frac{e^{-\kappa r}}{r}\sum_{k=0}^\infty (\kappa a_0)^{2k+2}\mathcal{C}_k,$$

$$\mathcal{C}_k = \frac{Z^{-1}}{(2k+3)!}\int_0^\infty \left(\frac{r_1}{a_0}\right)^{2k+2} 4\pi r_1^2\rho(r_1)\,dr_1. \quad \text{(B5)}$$

The coefficients $\mathcal{C}_k$ depend on the element specific density of shell electrons. The numerical values for the coefficients of the noble gases are listed in Table III. The sum in Eq. (B5) converges very fast. Therefore, only the first contribution needs to be taken into account, which leads to Eq. (41).

[1] J. L. Spitzer and R. Härm, Phys. Rev. **89**, 977 (1953).
[2] H. Brooks, Phys. Rev. **83**, 868 (1951); F. J. Blatt, Solid State Phys. **4**, 199 (1957).
[3] J. M. Ziman, Philos. Mag. **6**, 1013 (1961); T. E. Faber, *Introduction to the Theory of Liquid Metals* (Cambridge University Press, Cambridge, UK, 1972), Chap. 3.
[4] H. Reinholz, G. Röpke, S. Rosmej, and R. Redmer, Phys. Rev. E **91**, 043105 (2015).
[5] V. S. Karakhtanov, Contrib. Plasma Phys. **56**, 343 (2016).
[6] G. Röpke and R. Redmer, Phys. Rev. A **39**, 907 (1989).
[7] H. Reinholz, R. Redmer, and S. Nagel, Phys. Rev. E **52**, 5368 (1995).
[8] R. Redmer, Phys. Rep. **282**, 35 (1997).
[9] W. Ebeling and W. Richert, Ann. Phys. (Leipzig) **494**, 362 (1982).
[10] W. Ebeling, A. Förster, W. Richert, and H. Hess, Physica A **150**, 159 (1988).
[11] A. Förster, T. Kahlbaum, and W. Ebeling, Laser Part. Beams **10**, 253 (1992).
[12] S. Kuhlbrodt, B. Holst, and R. Redmer, Contrib. Plasma Phys. **45**, 73 (2005).
[13] S. Kuhlbrodt and R. Redmer, Phys. Rev. E **62**, 7191 (2000).
[14] S. Kuhlbrodt, R. Redmer, A. Kemp, and J. M.-t. Vehn, Contrib. Plasma Phys. **41**, 3 (2001).
[15] S. Kuhlbrodt, R. Redmer, H. Reinholz, G. Röpke, B. Holst,

V. B. Mintsev, V. K. Gryaznov, N. S. Shilkin, and V. E. Fortov, Contrib. Plasma Phys. **45**, 61 (2005).
[16] J. R. Adams, H. Reinholz, R. Redmer, V. B. Mintsev, N. S. Shilkin, and V. K. Gryaznov, Phys. Rev. E **76**, 036405 (2007).
[17] L. C. Pitchford, L. L. Alves, K. Bartschat, S. F. Biagi, M. C. Bordage, A. V. Phelps, C. M. Ferreira, G. J. M. Hagelaar, W. L. Morgan, S. Pancheshnyi, V. Puech, A. Stauffer, and O. Zatsarinny, J. Phys. D **46**, 334001 (2013).
[18] L. L. Alves, K. Bartschat, S. F. Biagi, M. C. Bordage, L. C. Pitchford, C. M. Ferreira, G. J. M. Hagelaar, W. L. Morgan, S. Pancheshnyi, A. V. Phelps, V. Puech, and O. Zatsarinny, J. Phys. D **46**, 334002 (2013).
[19] M. C. Bordage, S. F. Biagi, L. L. Alves, K. Bartschat, S. Chowdhury, L. C. Pitchford, G. J. M. Hagelaar, W. L. Morgan, V. Puech, and O. Zatsarinny, J. Phys. D **46**, 334003 (2013).
[20] R. Vanderpoorten, J. Phys. B **8**, 926 (1975).
[21] J. M. Paikeday, J. Chem. Phys. **65**, 397 (1976).
[22] S. Sur and A. S. Ghosh, Phys. Rev. A **25**, 2519 (1982).
[23] A. W. Pangantiwar and R. Srivastava, Phys. Rev. A **40**, 2346 (1989).
[24] M. Adibzadeh and C. E. Theodosiou, Atom. Data Nucl. Data Tab. **91**, 8 (2005).
[25] V. S. Karakhtanov, Plasma Phys. Rep. **33**, 232 (2006).
[26] D. Zubarev, V. Morozov, and G. Röpke, *Statistical Mechanics of Non-equilibrium Processes* (Akademie-Verlag, Berlin, 1997), Vol. 2.
[27] G. Röpke, *Non-equilibrium Statistical Physics* (Wiley-VCH, Weinheim, 2013).
[28] H. A. Gould and H. E. DeWitt, Phys. Rev. **155**, 68 (1967).
[29] C.-V. Meister and G. Röpke, Ann. Phys. (Leipzig) **494**, 133 (1982).
[30] G. Röpke, Phys. Rev. A **38**, 3001 (1988).
[31] S. Rosmej, Contrib. Plasma Phys. **56**, 327 (2016).
[32] R. Redmer, G. Röpke, and R. Zimmermann, J. Phys. B **20**, 4069 (1987).
[33] E. Clementi and C. Roetti, At. Data Nucl. Data Tables **14**, 177 (1974).
[34] M. Born and W. Heisenberg, Z. Phys. **23**, 388 (1924).
[35] J. M. Paikeday, Int. J. Quantum Chem. **40**, 569 (1991); **65**, 585 (1997); J. M. Paikeday and A. Longstreet, *ibid.* **70**, 989 (1998); J. M. Paikeday, *ibid.* **75**, 399 (1999); **80**, 989 (2000).
[36] C. Bottcher, J. Phys. B **4**, 1140 (1971).
[37] D. M. Schrader, Phys. Rev. A **20**, 918 (1979).
[38] M. H. Mittleman and K. M. Watson, Phys. Rev. **113**, 198 (1959).
[39] R. W. Crompton, M. T. Elford, and A. G. Robertson, Aust. J. Phys. **23**, 667 (1970).
[40] A. G. Robertson, J. Phys. B **5**, 648 (1972).
[41] C. Ramsauer and R. Kollath, Ann. Phys. **395**, 536 (1929).
[42] J. Townsend and V. Bailey, Philos. Mag. **43**, 593 (1922).
[43] H. B. Milloy, R. W. Crompton, J. A. Rees, and A. G. Robertson, Aust. J. Phys. **30**, 61 (1977).
[44] J. P. England and M. T. Elford, Aust. J. Phys. **41**, 701 (1988).
[45] T. Koizumi, E. Shirakawa, and I. Ogawa, J. Phys. B **19**, 2331 (1986).
[46] J. B. Furness and I. E. McCarthy, J. Phys. B **6**, 2280 (1973).
[47] M. E. Riley and D. G. Truhlar, J. Chem. Phys. **63**, 2182 (1975).
[48] A. W. Yau, R. P. McEachran, and A. D. Stauffer, J. Phys. B **11**, 2907 (1978).
[49] M. H. Mittleman and K. M. Watson, Ann. Phys. (NY) **10**, 268 (1960).
[50] S. Hara, J. Phys. Soc. Jpn. **22**, 710 (1967).
[51] W. M. Duxler, R. T. Poe, and R. W. LaBahn, Phys. Rev. A **4**, 1935 (1971).
[52] D. G. Thompson, Proc. Roy. Soc. London, Ser. A **294**, 160 (1966).
[53] M. S. Pindzola and H. P. Kelly, Phys. Rev. A **9**, 323 (1974).
[54] R. Redmer and G. Röpke, Phys. A (Amsterdam, Neth.) **130**, 523 (1985).
[55] H. B. Milloy and R. W. Crompton, Phys. Rev. A **15**, 1847 (1977).
[56] D. F. Register, S. Trajmar, and S. K. Srivastava, Phys. Rev. A **21**, 1134 (1980).
[57] J. F. Williams, J. Phys. B **12**, 265 (1979).
[58] D. F. Register and S. Trajmar, Phys. Rev. A **29**, 1785 (1984).
[59] J. C. Gibson, R. J. Gulley, P. S. Sullivan, S. J. Buckman, V. Chan, and P. D. Burrow, J. Phys. B **29**, 3177 (1996).
[60] R. Panajotović, D. Filipović, B. Marinković, V. Pejčev, M. Kurepa, and L. Vušković, J. Phys. B **30**, 5877 (1997).
[61] S. K. Srivastava, H. Tanaka, A. Chutjian, and S. Trajmar, Phys. Rev. A **23**, 2156 (1981).
[62] A. Danjo, J. Phys. B **21**, 3759 (1988).
[63] J. C. Gibson, D. R. Lun, L. J. Allen, R. P. McEachran, L. A. Parcell, and S. J. Buckman, J. Phys. B **31**, 3949 (1998).
[64] D. F. Register, L. Vušković, and S. Trajmar, J. Phys. B **19**, 1685 (1986).
[65] S. V. Dudin, V. E. Fortov, V. K. Gryaznov, V. B. Mintsev, N. S. Shilkin, and A. E. Ushnurtsev, in *Shock Compression of Condensed Matter*, edited by S. C. Schmidt, D. P. Dandekar, and J. W. Forbes, AIP Conference Proceedings Vol. 429 (AIP, New York, 1998), pp. 793–795; V. Y. Ternovoi, A. S. Filinov, A. A. Pyalling, V. B. Mintsev, and V. E. Fortov, in *Shock Compression of Condensed Matter*, edited by M. D. Furnish, N. N. Tadhani, and Y. Horie, AIP Conference Proceedings 620 (New York, 2002), pp. 107–110.
[66] V. E. Fortov, V. Y. Ternovoi, M. V. Zhernokletov, M. A. Mochalov, A. L. Mikhailov, A. S. Filimonov, A. A. Pyalling, V. B. Mintsev, V. K. Gryaznov, and I. L. Iosilevski, J. Exp. Theor. Phys. **97**, 259 (2003).
[67] Y. V. Ivanov, V. B. Mintsev, V. E. Fortov, and A. N. Dremin, Sov. Phys. JETP **44**, 112 (1976).
[68] N. S. Shilkin, S. V. Dudin, V. K. Gryaznov, V. B. Mintsev, and V. E. Fortov, Sov. Phys. JETP **97**, 922 (2003).
[69] V. B. Mintsev and V. E. Fortov, JETP Lett. **30**, 375 (1979).
[70] W.-D. Kraeft, D. Kremp, W. Ebeling, and G. Röpke, *Quantum Statistics of Charged Particle Systems* (Akademie-Verlag, Berlin, 1986).
[71] B. Militzer, Phys. Rev. B **79**, 155105 (2009).
[72] K. P. Driver and B. Militzer, Phys. Rev. B **91**, 045103 (2015).